THE JOURNAL OF GENE MEDICINE
J Gene Med 2015; **17**: 101–115.
Published online in Wiley Online Library (wileyonlinelibrary.com) **DOI:** 10.1002/jgm.2829

RESEARCH ARTICLE

Adeno-associated virus mediated delivery of an engineered protein that combines the complement inhibitory properties of CD46, CD55 and CD59

Derek Leaderer
Siobhan M. Cashman
Rajendra Kumar-Singh*

Department of Developmental, Molecular and Chemical Biology, Program in Genetics, Sackler School of Graduate Biomedical Sciences, Tufts University School of Medicine, Boston, MA, USA

*Correspondence to:
R. Kumar-Singh, Department of Developmental, Molecular and Chemical Biology, Program in Genetics, Sackler School of Graduate Biomedical Sciences, Tufts University School of Medicine, 136 Harrison Avenue, Boston, MA 02111, USA.
E-mail: rajendra.kumar-singh@tufts.edu

Received: 3 September 2014
Revised: 10 March 2015
Accepted: 22 April 2015

Abstract

Background A variety of disorders are associated with the activation of complement. CD46, CD55 and CD59 are the major membrane associated regulators of complement on human cells. Previously, we have found that independent expression of CD55, CD46 or CD59 through gene transfer protects murine tissues against human complement mediated attack. In the present study, we investigated the potential of combining the complement regulatory properties of CD46, CD55 and CD59 into single gene products expressed from an adeno-associated virus (AAV) vector in a soluble non-membrane anchored form.

Methods Minigenes encoding the complement regulatory domains from CD46, CD55 and CD59 (SACT) or CD55 and CD59 (DTAC) were cloned into an AAV vector. The specific regulatory activity of each component of SACT and DTAC was measured *in vitro*. The recombinant AAV vectors were injected into the peritoneum of mice and the efficacy of the transgene products for being able to protect murine liver vasculature against human complement, specifically the membrane attack complex (MAC), was measured.

Results SACT and DTAC exhibited properties similar to CD46, CD55 and CD59 or CD55 and CD59, respectively, *in vitro*. AAV mediated delivery of SACT or DTAC protected murine liver vasculature from human MAC deposition by 63.2% and 56.7%, respectively.

Conclusions When delivered to mice *in vivo* via an AAV vector, SACT and DTAC are capable of limiting human complement mediated damage. SACT and DTAC merit further study as potential therapies for complement mediated disorders when delivered via a gene therapy approach.

Keywords CD59; CD46; CD55; complement system; AAV; gene therapy

Introduction

The complement system is the humoral component of the innate immune system responsible for inactivating invading pathogens and maintaining tissue homeostasis [1]. As a result of its potency, the complement system is tightly regulated by a variety of soluble and membrane bound inhibitors of complement [1,2]. Inappropriate activation of complement has been associated with

a wide variety of inherited and acquired diseases, including autoimmune, inflammatory, hematological, neurodegenerative, cancer, ischemia/reperfusion injuries, organ transplantation and sepsis [2–4]. Furthermore, foreign surfaces present in biomaterials such as medical implants, hemodialysis filters and gene delivery systems trigger activation of complement [3]. Although acute activation of complement occurs in diseases such as sepsis or transplant rejection, the majority of disorders associated with activation of complement are chronic [e.g. age-related macular degeneration (AMD), paroxysmal nocturnal hemoglobinuria or rheumatoid arthritis] [2]. Many of the chronic diseases involving complement are caused by deficiencies in regulators of complement [2]. These deficiencies are primarily of the alternative pathway but can also involve the classical pathway, such as in hereditary angioedema or systemic lupus erythematosus (SLE) [5].

Activation of complement terminates in the formation of the membrane attack complex (MAC), a pore that disrupts the cell membrane and subsequently lyses the cell [6]. Elevated levels of MAC coupled with polymorphisms or mutations in complement regulators are found in patients with chronic diseases such as AMD, suggesting that failure at a variety of check points in complement activation are associated with disease pathogenesis [7]. In the case of AMD, individuals with a reduced ability to form MAC are partially protected from disease pathogenesis without significant complications, supporting the hypothesis that long-term attenuation of complement activation for chronic disorders may be a viable approach for the treatment of AMD and other complement-associated disorders such as rheumatoid arthritis [8,9].

Currently, there are only three Food and Drug Administration-approved inhibitors of complement available to patients, although there are over 25 different inhibitors of complement undergoing clinical trials [10]. In the context of chronic disorders such as AMD, this would require repeated injections of the complement inhibitor into the eye, a mode of delivery associated with significant side effects [11,12]. One alternative approach for the delivery of inhibitors of complement for chronic diseases such as AMD or rheumatoid arthritis is the use of somatic gene therapy. Although significant proof of principle has already been obtained demonstrating that gene therapy is efficacious in humans for the treatment of single gene disorders, patients with complex disorders such as rheumatoid arthritis have also been successfully treated using a gene therapy approach [13]. In some instances, the use of gene therapy has been found to be uniquely efficacious in mobilizing soluble versions of otherwise membrane-associated inhibitors of complement. For example, CD59 (protectin) is a naturally occurring inhibitor of MAC found tethered to the membranes of cells via a glycosylphosphatidylinositol (GPI) anchor. Although membrane-associated CD59 is a potent inhibitor of MAC, soluble membrane-independent CD59 has only been reported to be efficacious *in vivo* when delivered via a gene therapy vector such as adeno-associated virus (AAV) [14].

CD55 (decay accelerating factor) is a GPI anchored protein that regulates complement activity by accelerating the decay of the classical as well as the alternative C3 convertase [6]. CD46 (membrane cofactor protein) is a ubiquitously expressed type 1 transmembrane glycoprotein that acts as a cofactor for factor I mediated cleavage of C3b and C4b, preventing formation of the classical and alternative C3 convertase [15]. CD46 regulates the amplification loop of the alternative pathway of activation of complement. Although having differing properties, CD55 and CD46 each contain a series of 60 amino acid repeat motifs called short consensus repeats (SCR) that are considered to act as complement regulatory modules [16]. Species specificity between human and mouse complement proteins limit the testing of human complement inhibitors in murine tissues *in vivo* [17]. Previously, we have found that CD59, CD46 or CD55 expressed separately on the surface of murine cells can protect those cells from human complement mediated damage [18–20]. Each of the above molecules target a different component of activated complement. The goals of the present study were to examine whether a similar gene therapy approach may be utilized to deliver a single molecule containing all of the disparate properties of CD55, CD46 and CD59 or the combinatorial properties of CD55 and CD59.

Materials and methods

Cell lines

Hepa1c1c7 and HEK293 cell lines were obtained from ATCC and maintained in αMEM and Dulbecco's modified eagle's medium (DMEM), respectively, supplemented with 10% fetal bovine serum (FBS). The human embryonic retinoblast, 911, cell line was maintained in DMEM supplemented with 10% FBS [21]. Cell culture reagents were purchased from Invitrogen Life Technologies (Carlsbad, CA, USA) and cells were maintained in a humidified incubator at 37°C with 5% CO_2.

Structure and synthesis of soluble active complement terminator (SACT) and dual terminator of active complement (DTAC)

A cDNA was synthesized by GenScript (Piscataway, NJ, USA) to encode SACT, which contains the sequence encoding the human CD59 (ATCC catalog. no. 10658204)

DOI: 10.1002/jgm

secretory peptide followed by the coding sequence for amino acids 34–296 of human CD46 (ATCC catalog. no. 7491463) encoding the four SCR domains of CD46 (Figure 1A) [22]. The human CD46 sequence is attached via a sequence encoding a five glycine linker to a sequence encoding amino acids 33–356 of human CD55 (ATCC catalog. no. 5830488), which comprise the SCR domains and STP region of CD55 [16]. An additional sequence encoding a five glycine linker attaches the STP region of CD55 to a sequence encoding the 76 amino acid functional domain of human CD59. A cDNA encoding the DTAC was also synthesized by GenScript to contain the sequence encoding the human CD59 secretory peptide followed by the coding sequence for amino acids 33–356 of human CD55 (as described above) (Figure 1A). The sequence encoding the STP region of CD55 sequence was attached via a sequence encoding a five glycine linker to a sequence encoding the 76 amino acid functional domain of human CD59. The cDNAs encoding SACT and DTAC were cloned into the *Xho*I and *Eco*RV sites of pAAVCAG, a modified version of pAAV-MCS (Stratagene, La Jolla, CA, USA) containing a chicken β-actin promoter/CMVenhancer (CAG) and a rabbit globin polyadenylation signal (generously provided by C. Cepko and T. Matsuda, Osaku University, Japan) to generate pAAV2CAGSACT and pAAV2CAGDTAC, respectively.

Construction of AAV constructs

Recombinant AAV was generated via triple transfection of 293 cells with each of pAAV2CAGSACT, pAAV2CAGDTAC and pAAV2CAGGFP, pHelper (Stratagene) and pAAV2/8Rep/Cap [14]. The resulting AAV vectors, AAV2/8SACT, AAV2/8DTAC and AAV2/8GFP were purified by iodixanol gradient and dialyzed in Ringer's lactate buffer [23]. Viral genomes were titered by real-time quantitative polymerase chain reaction using primers targeting AAV2 inverted terminal repeats as described previously [24].

Western blot analysis

The human embryonic retinoblast, 911, cell line was transfected with pAAV2CAGDTAC, pAAV2CAGSACT or

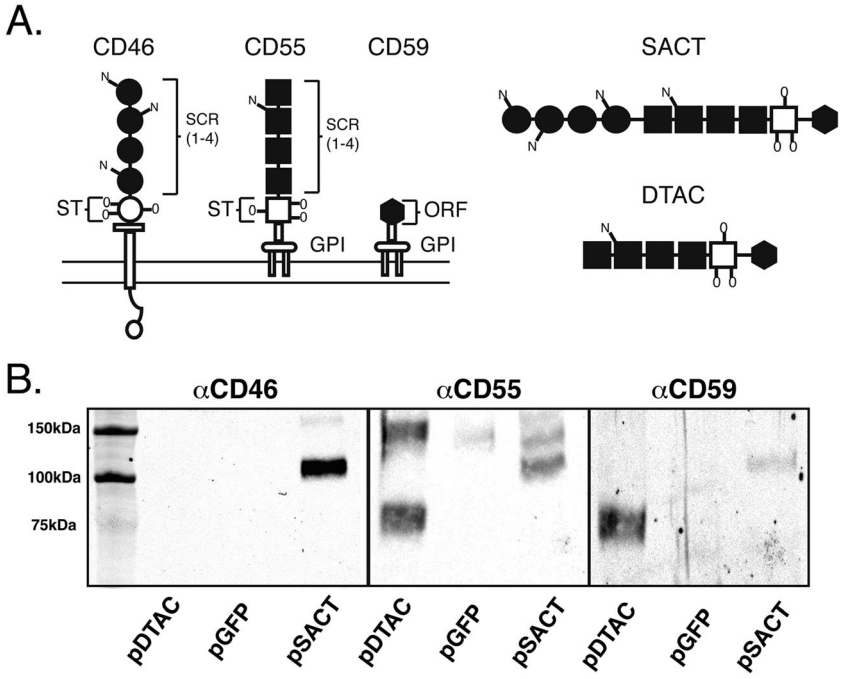

Figure 1. Structure and expression of SACT and DTAC. (A) Schematic of the structure of the human membrane-associated complement regulators, CD46, CD55 and CD59 and the soluble recombinant proteins, SACT and DTAC. Both CD55 and CD46 each contain four SCR domains and a serine/threonine (S/T) rich region. The SCR and S/T domains are sites of N- and O-linked glycosylation, respectively. CD46 inserts in the membrane via a hydrophobic domain, whereas CD55 and CD59 each attach to the membrane via a GPI anchor. CD59 contains a short functional unit of 76 amino acids. Both SACT and DTAC contain the four SCR domains and the S/T-rich region of human CD55 separated by a poly glycine linker from the functional domain of human CD59. SACT additionally contains the four SCR domains of human CD46 at the N-terminus separated by a polyglycine linker from the SCRs of CD55. Both SACT and DTAC contain a secretory signal derived from human CD59. The membrane-spanning domain of CD46 and the signals for attachment of a GPI-anchor to each of CD55 and CD59 were not included in the recombinant proteins. (B) Western blot showing media from cells transfected with pDTAC, pGFP or pSACT probed with antibodies against CD46, CD55 and CD59.

DOI: 10.1002/jgm

pAAV2CAGGFP using Lipofectamine 2000 in accordance with the manufacturer's instructions (Invitrogen). Seventy-two hours post-transfection, media was collected, centrifuged and electrophoresed on a 10% Tris-HCl gel and proteins subsequently transfered to a nitrocellulose membrane, probed with a mouse anti-human CD46 antibody (MEM258; Serotec, Raleigh, NC, USA) at a dilution of 1:10 000, a goat anti-human CD55 antibody (AF2009; R&D systems, Minneapolis MN, USA) at a dilution of 1:20 000 or a rabbit anti-human CD59 antibody (ab124396; Abcam, Cambridge, MA, USA) at a dilution of 1:5000. An IRDye linked secondary antibody was used followed by detection with the Odyssey Li-Cor System (Li-Cor Biosciences, Lincoln, NB, USA).

Complement assays with Hepa1c1c7 cells

For FACS analyses, hepa1c1c7 cells were plated in αMEM/2% FBS without phenol red at 50% confluency. After 3 days, the hepa1c1c7 cells were collected by trypsinization (0.25% ethylenediaminetetraacetic acid) and resuspended in 1X phosphate-buffered saline (PBS) containing 0.5% FBS. 5×10^5 cells were centrifuged at 335 g at 4°C and resuspended in 500 μl of media from 911 cells transfected with pDTAC, pSACT or pGFP. Normal human serum (NHS; Complement Technology, Tyler, TX, USA) or heat-inactivated (hi; 56°C for 1 h) NHS was added to each sample to a final concentration of 1% and samples were incubated with constant rotary motion at 37 °C for 1 h. Cell lysis was determined using the propidium iodide (PI) exclusion method. Next, 1 μl of PI (2 mg/ml) was added to each sample and 25 000 cells were counted by FACS (FACS Calibur) for PI uptake (CellQuest Pro software; Becton-Dickinson, Franklin Lakes, NJ, USA).

For *in vitro* MAC deposition, 35 000 hepa1c1c7 cells were seeded per well of an eight-well chamber slide (Becton Dickinson) in αMEM/2% FBS. Twenty-four hours later, media was removed and the cells were washed three times with 1 × PBS and cells incubated with 10% NHS or heat inactivated NHS (hiNHS) resuspended in media from 911 cells transfected with either pDTAC, pSACT or pGFP for 10 min at 37°C. Cells were then washed twice with cold 1 × PBS and then fixed for 15 min with 3.7% formaldehyde. Cells were stained for MAC deposition as described below.

Hemolytic assays

Sensitized sheep erythrocytes (Complement Technology) were washed twice with Gelatin Veronal Buffer (GVB^{2+}) and suspended to a concentration of 5×10^8 cells/ml. Next, 25 μl of erythrocyte suspension was used per reaction. Then, 125 μl of media from either pGFP-, pDTAC- or pSACT-transfected 911 cells containing NHS to a final concentration of 0.3% was added to the erythrocyte suspension. After 1 h of incubation at 37°C, erythrocytes were centrifuged (500 ***g*** for 4 min at 4°C) and absorbance of the supernatant was read at 405 nm (Filter Max F5 multi-mode microplate reader, Molecular Devices; Sunnyvale, CA, USA).

For CD55 blocking assays, media from either pGFP-, pDTAC- or pSACT-transfected 911 cells that had been incubated with or without anti-CD55 antibody (ab33111; Abcam) at room temperature for 30 min was added to the erythrocytes along with 0.3% NHS. After 1 h of incubation at 37°C, supernatant was collected and absorbance was read as above.

For C9-incorporation assays, suspended erythrocytes were incubated with 0.1% C9-depleted serum (Complement Technology) for 1 h at 37°C to permit formation of the C5b-8 complex. After washing twice with GVB^{2+}, media from either pGFP-, pDTAC- or pSACT-transfected 911 cells that had been pre-incubated on ice for 30 min in the presence or absence of 0.04 μg/ml C9 (Complement Technology) was added. After 30 min of incubation at 37°C, samples were centrifuged and absorbance was determined, as described previously [25]. All hemolytic assays were normalized to the lysis of erythrocytes in media from pGFP-transfected cells (set at 100% lysis).

Factor I cofactor activity

In vitro cofactor activity was assayed as described previously [26]. Media from either pGFP-, pDTAC- or pSACT-transfected 911 cells was incubated with 3 μg of C3b, plus 100 ng of factor I in a total volume of 20 μl at 37°C for 4 h. Reactions were terminated by adding 5 μl of sodium dodecyl sulfate/polyacrylamide gel electrophoresis (SDS-PAGE) sample buffer containing β-mercaptoethanol and boiling. C3b reaction products were analyzed by Western blot using a 10% SDS-PAGE gel. After transfer, membrane was probed with polyclonal goat anti-human C3 (A213, Complement Technology) at a dilution of 1:1000. The intensity of the signal of the C3b (α chain, 104 kDa) remaining following incubation with factor I in the presence of conditioned media was measured (see below). To account for sample loading errors, the signal intensity of the C3b (α chain) was normalized using the signal intensity of the uncleaved β chain of C3b.

Degradation of alternative pathway C3 convertase

Microtiter plates were coated with 0.1% agarose in water and allowed to dry for 36 h at 37°C, after which the wells

DOI: 10.1002/jgm

were blocked with 1% bovine serum albumin in PBS for 2 h at room temperature as described previously [25]. NHS diluted in Mg^{2+}EGTA was added to the agarose-coated plate and incubated at 37°C for 1 h. After washing, media from either pGFP-, pDTAC- or pSACT-transfected 911 cells was added to the plate after which the plates were incubated at 37°C for 1 h. Factor B remaining bound to the plate was then detected using a factor B (A235; Complement Technologies) specific antibody followed by horseradish peroxidase-conjugated secondary antibody.

In vivo liver MAC deposition assay

This protocol has been described in detail previously [27]. Animal use in the present study was in accordance with the ARVO Statement for the Use of Animals in Ophthalmic and Vision Research. This study was approved by Tufts University Institutional Animal Care and Use Committee (IACUC) protocol B2011-150. Briefly, 6–10-week-old C57BL/6 J mice were injected intraperitoneally with 3.3×10^{11} genome copies of AAV2/8DTAC, AAV2/8 SACT or AAV2/8polyA. After 3 weeks, mice were injected intracardially with 200 μg of anti-mouse PECAM antibody (clone 2H8, 1.4 mg/ml, prepared as described previously). After 4–6 h of incubation, mice underwent a cardiac perfusion of 1 ml of GVB^{2+} followed by 1.5 ml of 90% NHS (Complement Technology) in GVB^{2+}. After 15 min of incubation at 37°C, the median lobe of the liver was harvested and fixed overnight in 4% paraformaldehyde at 4°C. Cryosections (8 μm) were obtained and stained for MAC as described below. Imaging was performed using an IX51 microscope (Olympus, Tokyo, Japan) equipped with a Retiga 2000r camera (QImaging, Surrey, BC, Canada). Intensity of MAC staining over the entire section as well as around the vessels was quantified using ImageJ (National Institutes of Health, Bethesda, MD, USA). Large blood vessels were defined as those with a diameter larger than two cell widths and include arteries, arterioles, veins and venules but exclude capillaries and sinusoids. The outer and inner boundaries of the large blood vessels were traced using the free-hand selection tool and total intensity and total area was calculated for each using the measure function. Average vessel intensity was calculated as:

$$X = [I_{\text{outer}} - I_{\text{inner}}]/[A_{\text{outer}} - A_{\text{inner}}]$$

Immunohistochemistry

To detect MAC deposition on hepa1c1c7 cells, cells were incubated for 2.5 h at room temperature with mouse anti-human C5b-9 (dilution 1:100) (ab66768; Abcam) in 0.05% triton containing 6% normal goat serum (NGS). Cy3 conjugated goat anti mouse (dilution 1:200) in 0.05% triton containing 3% NGS for 1 h at room temperature was used for secondary detection. For detection of MAC deposition on liver vasculature, liver sections were incubated for 2.5 h at room temperature with rabbit anti-human C5b-9 (Complement Technology) (dilution 1:400) in 0.5% triton, after 1 h of blocking with 6% normal goat serum (NGS) and 0.5% triton. Cy3-conjugated goat anti-rabbit (dilution 1:200) was used for 1 h at room temperature for secondary detection.

Images were captured using an IX51 microscope and ImageJ software was used to quantify fluorescence. Raw fluorescence units were measured and background for each image was subtracted.

Statistical significance was determined for all assays using two-tailed unpaired *t*-tests and all statistical analyses were performed using Prism, version 5.0a (GraphPad Software Inc., La Jolla, CA, USA).

Results

Synthesis of SACT and DTAC

We generated a plasmid containing an expression cassette for SACT. SACT is comprised of an engineered DNA sequence designed to express a protein composed of the four SCR domains of human CD46 separated by a polyglycine linker from the four SCR domains and serine/threonine (S/T)-rich region of human CD55. An additional polyglycine linker separates the S/T-rich region of CD55 from the functional domain (amino acids 1–76) of human CD59 (Figure 1A). The N-terminus of SACT contains a secretory signal derived from the native human CD59. The membrane-spanning domain of CD46 and the signals for attachment of a GPI-anchor to each of CD55 and CD59 were not included in the recombinant protein such that unlike its individual components, SACT would not anchor to the plasma membrane (Figure 1A).

As a result of concerns that SACT may not fold and hence function correctly, we also generated a smaller recombinant protein, DTAC, a protein engineered to contain the four SCR domains and S/T-rich region of human CD55 separated by a poly glycine linker from the functional domain (as described above) of human CD59. As for SACT, DTAC contains the secretory peptide of human CD59 (Figure 1A). DTAC was also rendered membrane-independent by omission of CD55 and CD59 signal peptides for attachment of a GPI-anchor.

Because we aimed to express SACT *in vivo* using a gene therapy approach, a cDNA encoding SACT was inserted into the plasmid, pAAVCAG, containing AAV2 inverted terminal repeats to generate pSACT [14]. As a negative

DOI: 10.1002/jgm

control, we utilized the same construct devoid of the SACT cDNA, referred to as pAAVCAG. A cDNA encoding DTAC was inserted into pAAVCAG for expression from an AAV2 virus, generating pDTAC.

SACT and DTAC are secreted proteins

The predicted molecular weight of SACT and DTAC proteins are 76 kDa and 47 kDa, respectively (Serial Cloner, version 2.6.1; Serial Basic Software; http://serialbasics.free.fr). SACT retains three of the N-linked glycosylation sites of CD46 and both SACT and DTAC retain one N-linked and three O-linked glycosylation sites of CD55 [16,28]. These modifications are predicted to increase the molecular weight of DTAC by approximately 29 kDa [28] and SACT by approximately 37 kDa (8 kDa + 29 kDa) [16], to yield recombinant proteins of 76 kDa and 113 kDa, respectively. Western blot analyses of media from pSACT-transfected human embryonic 911 retinoblasts probed with antibodies against either CD46, CD55 or CD59 indicated a protein band of approximately 110 kDa, which is consistent with the predicted molecular weight of glycosylated SACT. As expected, this band was absent in media from pGFP or pDTAC transfected cells (Figure 1B) [21]. Similarly, western blot analyses of pDTAC-transfected cells probed with the above antibodies indicated the presence of an approximately 76 kDa band, consistent with the predicted molecular weight of glycosylated DTAC. As expected, this band was absent in media from cells transfected with pGFP or pSACT (Figure 1B). As also expected, the 76-kDa protein is only observed when probed with antibodies against CD55 and CD59 and shows no reactivity to antibody against CD46 (Figure 1B). We conclude that SACT and DTAC are secreted and contain the expected combination of complement regulatory domains and glycosylation sites.

SACT acts as a co-factor for factor I mediated cleavage of C3b

Spontaneous 'tickover' of the alternative pathway of the complement system results in the formation of C3b on cell surfaces [6]. The amount of C3b present is regulated by proteolytic cleavage of C3b by the serine protease factor I. Factor I cleaves the 104-kDa α' chain of C3b into inactivated 67-kDa $iC3b_H$ and 42-kDa $iC3b_L$ chains, respectively (Figure 2A) [15]. CD46 functions as a co-factor for factor I, thus accelerating the formation of $iC3b_H$ and $iC3b_L$, although it has been shown that factor I alone can cleave C3b. To determine whether SACT exhibits co-factor properties similar to CD46, we incubated 3 μg of C3b in media prepared from 911 cells transfected with either pSACT, pDTAC or pGFP. Incubations were performed in the presence or absence of 100 ng of factor I [14]. The relative amount of 104-kDa α' chain of C3b remaining after 4 h of incubation was examined by quantitative western blot using a polyclonal anti-C3 antibody (Figure 2B). The uncleaved β chain of C3b was used to normalize the data. Media from pSACT-transfected cells containing C3b and factor I led to a 51.8 ± 10.5% ($p = 0.007$) reduction in the amount of the 104-kDa α' chain of C3b relative to media from pGFP-transfected cells containing C3b and factor I, and a 46.2 ± 4.8% ($p = 0.0007$) reduction relative to media from pDTAC-transfected cells containing C3b and factor I (Figure 2C). There was no significant difference ($p = 0.34$) between the amount of 104-kDa α' chain of C3b exposed to the media of pGFP and pDTAC transfected cells containing C3b and factor I, as expected (Figure 2C). We conclude that similar to CD46, SACT can act as a cofactor for factor I mediated cleavage of C3b.

SACT and DTAC accelerate degradation of the C3-convertase

Binding of factor B to membrane associated C3b results in the formation of the C3 convertase [6]. CD55 can both prevent binding of factor B to C3b, and cause dissociation of factor B from C3b, thereby reducing the amount of C3 convertase available for further activation of complement (Figure 3A) [6]. To determine whether SACT or DTAC could dissociate Factor B from C3b, thus reducing C3 convertase activity, we quantified the amount of factor B remaining in association with C3b immobilized on agarose when incubated in the presence of SACT or DTAC. Agarose-coated microtiter plates were incubated with NHS in the presence of Mg^{2+}EGTA to allow formation of the alternative pathway C3 convertase. The wells were subsequently incubated with media from either pSACT-, pDTAC- or pGFP- transfected 911 cells. The amount of factor B associated with the agarose-bound C3b after 1 h at 37°C was determined by antibody staining for factor B following several washes to remove unbound factor B. Quantification of Factor B staining indicated that relative to media from pGFP- transfected 911 cells, media from pDTAC- or pSACT-transfected cells resulted in a 16.1 ± 6.4% ($p = 0.0214$) and 16.8 ± 6.1% ($p = 0.0127$) reduction in C3b-bound factor B, respectively (Figure 3B). We conclude that, similar to CD55, DTAC and SACT accelerate the decay of the C3 convertase.

Although the effects of SACT and DTAC on degradation of C3-convertase are comparable to those observed for native complement inhibitors using this assay [25], the low level of reduction in C3-convertase by STAC and DTAC relative to the control led us to further validate function of the CD55-derived SCRs using a CD55-blocking hemolytic

DOI: 10.1002/jgm

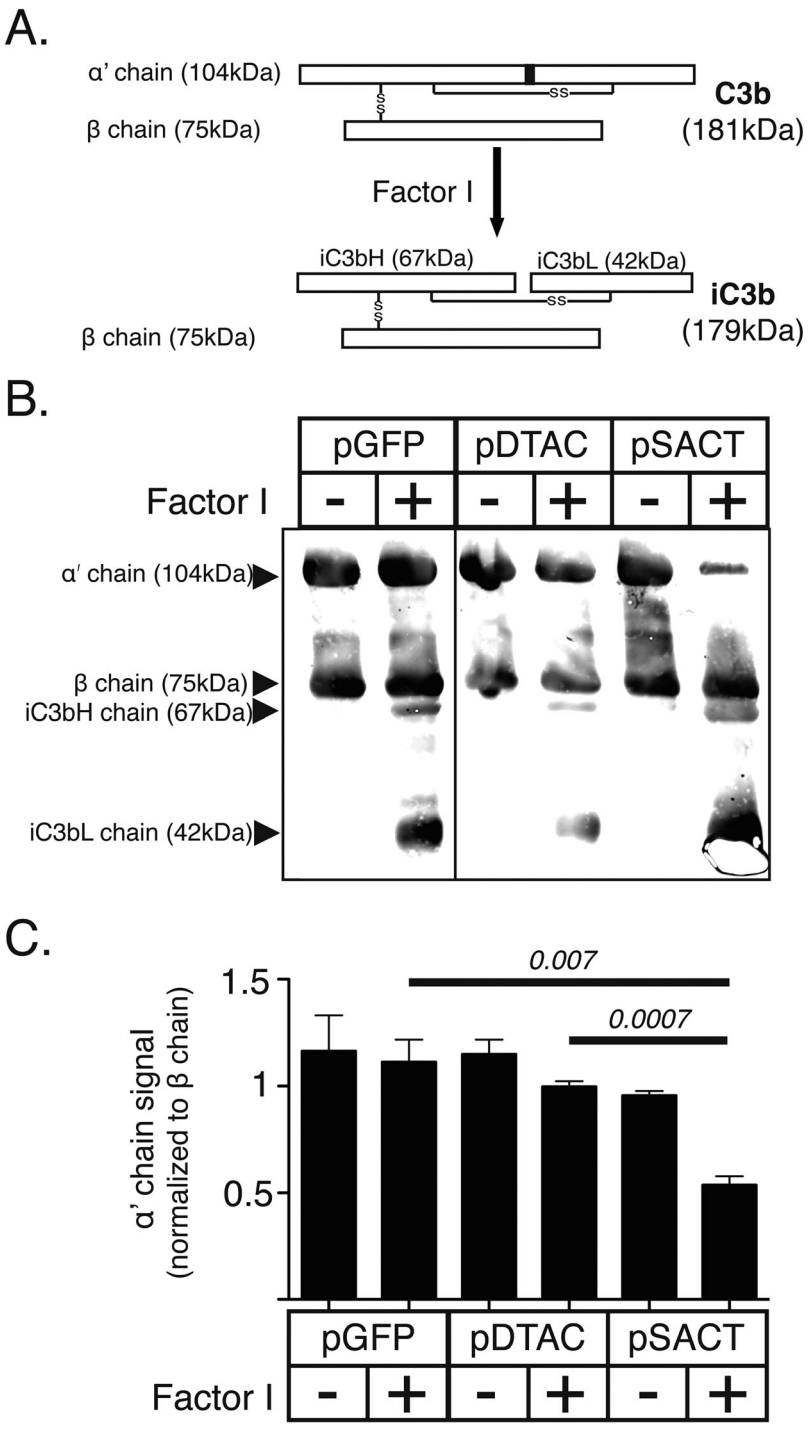

Figure 2. SACT acts as a co-factor for factor I mediated cleavage of C3b. (A) Schematic of factor I cleavage of C3b. C3b consists of two polypeptide chains (α' and β), joined by a disulfide linkage. Factor I mediates cleavage of the 104 kDa α' chain into the inactive fragments, iC3bH and iC3bL. (B) Schematic showing CD46 binding of C3b deposited on the cell membrane to act as a co-factor for factor I-mediated cleavage to inactive iC3b. (C) Western blot of purified C3b incubated in media from cells transfected with either pSACT, pDTAC or pGFP in the presence or absence of factor I and probed with an antibody against C3 confirms increased cleavage of the α' chain in the presence of media from cells transfected with pSACT relative to that occurring in the presence of either pGFP or pDTAC. (D) Quantification of western blot data showing a 51.8 ± 10.5% ($p = 0.007$) and 46.2 ± 4.8% ($p = 0.0007$) reduction in the amount of the α' chain of C3b in media from pSACT-transfected cells containing C3b and Factor I relative to media from pGFP-transfected cells and pDTAC-transfected cells containing C3b and factor I, respectively. Note: signal intensities for the α' chain were normalized to the signal intensity of the β chain. The experiment was performed independently three times. Western blot images are taken from the same gel and rearranged for presentation.

DOI: 10.1002/jgm

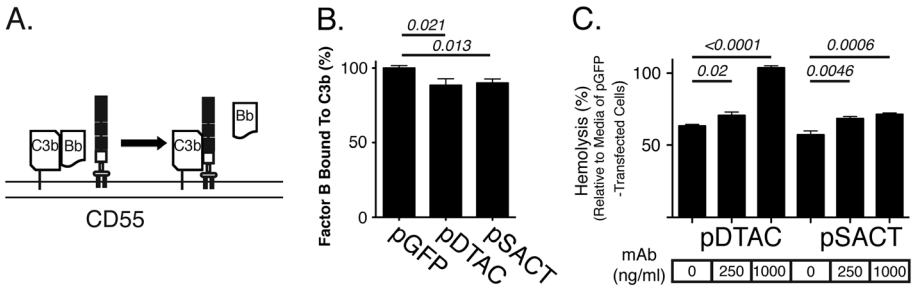

Figure 3. SACT and DTAC accelerate degradation of C3 convertase. (A) Schematic of CD55 dissociation of factor B binding to C3b to accelerate degradation of the C3 convertase. (B) Quantification of immunostaining of factor B binding to agarose-bound C3b using an antibody against factor B shows that media from pDTAC- or pSACT-transfected cells resulted in a 16.1 ± 6.4% ($p = 0.0214$, $n = 11$) and 16.8 ± 6.1% ($p = 0.0127$, $n = 11$) reduction in C3b-bound factor B, respectively, relative to media from pGFP-transfected cells ($n = 10$). Note: factor B binding is presented as percentage staining relative to the average staining intensity of factor B bound to C3b in the presence of media from pGFP-transfected cells. The experiment was repeated twice independently. (C) Quantification of human complement-mediated lysis of sheep erythrocytes incubated with media from cells transfected with either pDTAC or pSACT in the presence or absence of CD55 blocking antibody. A significant reduction in protection against cell lysis is observed for both DTAC and SACT in the presence of antibody. The experiment was conducted twice in triplicate.

assay. We quantified human complement-mediated lysis of sensitized sheep erythrocytes in the presence of media from either pSACT- or pDTAC-transfected 911 cells in the presence of CD55 blocking antibody. At an antibody concentration of 1 μg/ml, the ability of media from pDTAC- and pSACT-transfected cells to protect sheep erythrocytes from human complement was reduced by 40.42% ± 1.84% ($p < 0.0001$) and 14.18% ± 2.88% ($p = 0.0006$), respectively, relative to media from transfected 911 cells without blocking antibody (Figure 3C). At lower concentrations (250 ng/ml) of blocking antibody, the ability of media from pDTAC- and pSACT-transfected cells to protect sheep erythrocytes from lysis was reduced by 7.33% ± 2.66% ($p = 0.02$) and 11.2% ± 3.09% ($p = 0.0046$), respectively, relative to media from transfected cells without blocking antibody (Figure 3C). There was no reduction in hemolysis when media from pDTAC was incubated with 1 μg/ml anti-CD55 antibody, suggesting that there was no effect from the CD59 component of DTAC. This was likely a result of the concentration of serum used (0.3%). In titration experiments, we have observed a loss of CD59 inhibition at concentrations of human serum where CD55 inhibition can be measured (Sweigard, H; Cashman, SM; Kumar-Singh, R). That a similar ablation of hemolysis inhibition was not observed for SACT was likely a result of the presence of the CD46 moiety. We hence conclude that the CD55-derived SCRs in SACT and DTAC are functionally active.

SACT and DTAC attenuate recruitment of C9 into the MAC

Formation of the MAC begins with the assembly of the C5b-8 complex on the cell membrane, followed by the recruitment and polymerization of multiple units of C9 to form the lytic pore known as MAC [6]. CD59 acts as an inhibitor of MAC formation by preventing the recruitment and polymerization of C9 (Figure 4A) [2]. To determine whether the CD59 module of SACT or DTAC can attenuate recruitment of C9 into MAC, we incubated antibody-sensitized sheep erythrocytes with C9-depleted NHS to permit assembly of the C5b-8 complex on the cell surface. We subsequently added purified C9 protein with media from either pDTAC- or pSACT-transfected 911 cells and indirectly measured formation of the MAC through quantification of hemoglobin released as a result of lysis of the sheep erythrocytes. We found that media from pDTAC- and pSACT-transfected 911 cells reduced the release of hemoglobin from sheep erythrocytes by 34.81 ± 3.6% ($p < 0.0001$) and 29.9 ± 4.6% ($p < 0.0001$), respectively, relative to erythrocytes incubated with NHS in the presence of media from pGFP-transfected cells (Figure 4B). We conclude that DTAC and SACT can attenuate the recruitment of C9 into the MAC, a property consistent with the presence of functional CD59.

SACT and DTAC attenuate human complement-mediated lysis of hepatocytes *in vitro*

To determine whether DTAC or SACT may protect sheep erythrocytes from NHS mediated cell lysis, we incubated immunoglobulin G-sensitized sheep erythrocytes in NHS pre-conditioned with media from pDTAC, pSACT or pGFP transfected 911 cells. pDTAC and pSACT transfected media reduced NHS mediated lysis of sheep erythrocytes by 47 ± 2.9% ($p < 0.0001$) and 21.5 ± 2.8% ($p < 0.0001$), respectively (Figure 5A), relative to pGFP transfected media, suggesting that DTAC and SACT can attenuate NHS

DOI: 10.1002/jgm

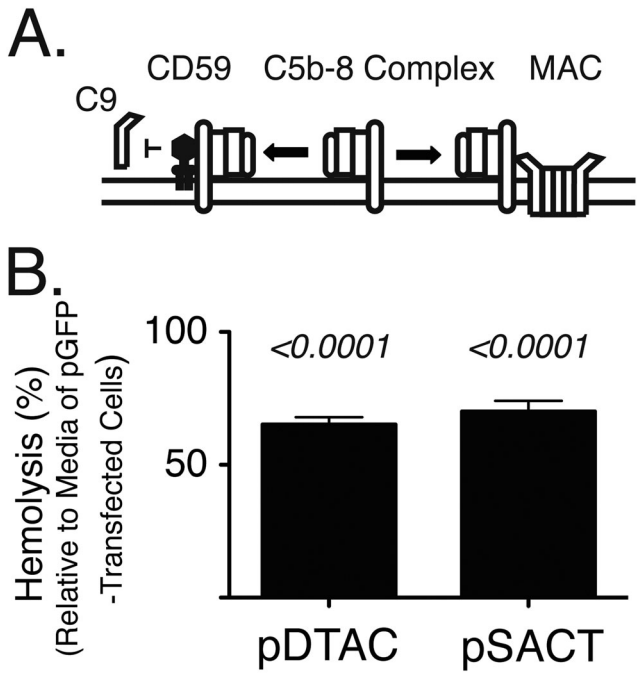

Figure 4. SACT and DTAC inhibit incorporation of C9 into the MAC. (A) Schematic of CD59 function. CD59 binds to the membrane-associated C5b-8 protein complex, preventing incorporation of C9 and formation of the MAC. MAC forms a pore on the cell surface, reducing integrity of the membrane. (B) Quantification of lysis of sheep erythrocytes by C9-depleted human serum incubated with C9 in the presence of media transfected with either pGFP, pDTAC or pSACT. Media from pDTAC- and pSACT-transfected cells reduced human complement-mediated lysis of erythrocytes by 34.81 ± 3.6% ($p < 0.0001$) and 29.9 ± 4.6% ($p < 0.0001$), respectively, relative to erythrocytes incubated in the presence of media from pGFP-transfected cells. The experiment was repeated three times in triplicate.

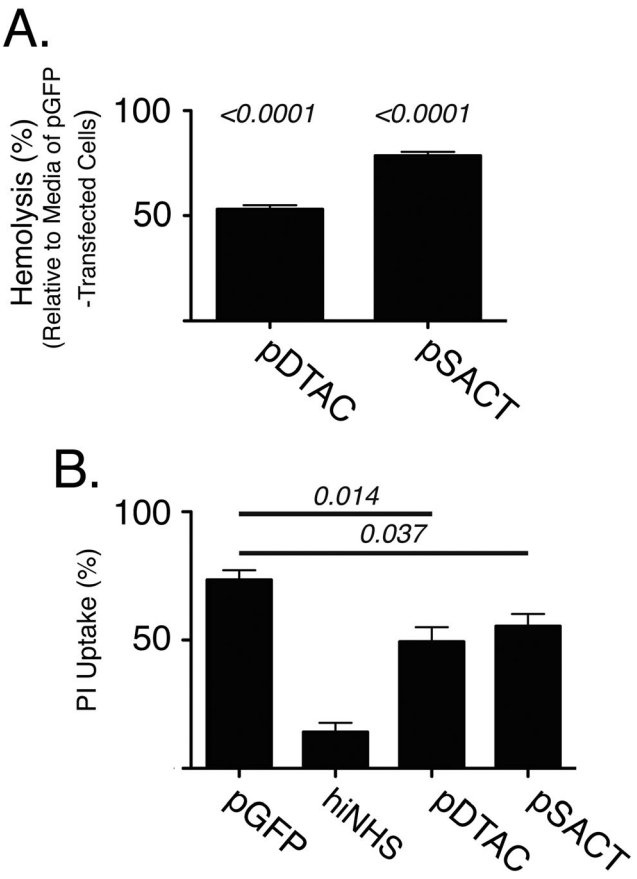

Figure 5. SACT and DTAC protect both sheep erythrocytes and murine hepatocytes from human complement-mediated lysis *in vitro*. (A) Quantification of lysis of sheep erythrocytes (hemolysis) by human serum in the presence of media from cells transfected with either pGFP, pDTAC or pSACT shows a 47 ± 2.9% ($p < 0.0001$) and 21.5 ± 2.8% ($p < 0.0001$) reduction in lysis by DTAC and SACT, respectively, relative to media from GFP-transfected cells. The experiment was repeated twice ($n = 5$ for condition). (B) Quantification of PI uptake by murine hepatocytes incubated with NHS in the presence of media from cells transfected with either pGFP, pDTAC or pSACT. A control experiment of hepatocytes incubated with hiNHS in the presence of media from pGFP-transfected cells is also shown. Relative to hepatocytes incubated with media from pGFP-transfected cells ($n = 7$), hepatocytes incubated with media from either pDTAC- or pSACT-transfected cells had a 28.73% ± 10.21% ($p = 0.014$, $n = 8$) or 20.8 ± 9.0% ($p = 0.037$, $n = 8$) reduction in PI uptake, respectively. The experiment was performed independently three times.

mediated cell lysis. Complement mediated attack of transplanted organs, such as the liver and kidney, is considered a primary cause of transplant rejection [29]. To determine whether SACT and DTAC can protect hepatocytes from human complement attack, murine hepa-1c1c7 cells were incubated in media from either pDTAC-, pSACT- or pGFP-transfected 911 cells containing NHS or hiNHS to a final concentration of 1%. Cell lysis was quantified by FACS analysis of PI uptake. A total of 73.52 ± 3.79% of cells was lysed when hepa-1c1c7 cells were incubated in NHS pre-conditioned with media from pGFP-transfected cells (Figure 5B). By contrast, 49.34 ± 5.7% and 55.48 ± 4.77% of cells were lysed when the NHS was pre-conditioned with media from DTAC or SACT, respectively, resulting in a 28.73% ± 10.21% ($p = 0.014$) or 20.8 ± 9.0% ($p = 0.037$) reduction in NHS mediated cell lysis attributable to DTAC and SACT, respectively (Figure 5B). This result indicates that DTAC and SACT can protect murine hepatocytes from human complement mediated attack.

DTAC and SACT reduce formation of the MAC *in vitro*

To determine whether DTAC or SACT-mediated reduction in lysis of hepatocytes was consistent with a reduction in formation of the MAC on the cell membrane, we incubated murine hepa1c1c7 cells in media from pGFP-, pDTAC- or pSACT-transfected 911 cells containing 10% NHS. Cells were subsequently fixed and stained with antibody against

DOI: 10.1002/jgm

human C5b-9 and staining intensity quantified using ImageJ (Figure 6A). We found that, relative to media from pGFP-transfected cells, media from pDTAC- and pSACT-transfected cells resulted in a 53.8 ± 10.37% ($p = 0.0004$) and 67.8 ± 9.15% ($p < 0.0001$) reduction in MAC deposition on murine hepatocytes, respectively (Figure 6B). We conclude that DTAC and SACT-mediated reduction of cell lysis is consistent with a reduced formation of the MAC on the surface of cells.

SACT and DTAC protect murine liver from human MAC deposition *in vivo*

A number of complement-mediated pathologies, including organ transplant rejection, have been shown to involve endothelial cells [2,29,30]. To overcome the limitation of testing the ability of human complement regulators to protect murine endothelium from complement attack *in vivo*, we have recently developed an *in vivo* model of human MAC deposition on murine liver vascular endothelium [27]. In this model, murine vascular endothelium is primed for complement attack by intracardial injection of an antibody against murine platelet/cell adhesion molecule (mPECAM-1). This is followed by perfusion with PBS to replace the blood and a subsequent perfusion with 90% NHS. Using this model, we have previously shown that adenovirus mediated expression of human soluble CD59 can inhibit deposition of human MAC on murine liver [27].

To examine whether SACT or DTAC can protect murine liver vasculature from human MAC deposition, we used each of the pSACT, pDTAC, and pGFP plasmids to generate a recombinant AAV serotype 2 pseudotyped with AAV serotype 8 capsid for each recombinant protein. An AAV2/8 construct devoid of a transgene has previously been described [14]. These vectors are referred to as AAV2/8SACT, AAV2/8DTAC, AAV2/8GFP and AAV2/8polyA, respectively.

To examine the tropism of AAV2/8 in murine liver, we injected 3.3×10^{11} genome copies of AAV2/8GFP into the peritoneum of 6–8-week-old C57BL/6 J mice. After 3 weeks, mice were sacrificed, livers harvested and cryosections examined for GFP expression. We found that GFP expression from AAV2/8GFP was observed throughout the liver, including cells proximal to blood vessels and sinusoids (Figure 7A). These results contrast our previous studies utilizing an adenovirus vector expressing GFP from the same CAG promoter, in which we observed GFP expression almost exclusively in the capsule of the liver following intraperitoneal delivery of the vector [27].

Having confirmed efficient transduction of murine liver with AAV2/8GFP, mice were injected intraperitoneally with a similar titer of AAV2/8DTAC, AAV2/8SACT or AAV2/8polyA. Three weeks post-injection with AAV, the mice were administered an intracardial injection of mPECAM-1, followed 4–6 h later by perfusion with 90% NHS. After 15 min, the livers were harvested for cryosectioning and stained for human MAC using antibody against C5b-9 (Figures 7B and 8A). As expected, MAC staining was observed in the blood vessels and sinusoids of the livers of mice injected with AAV2/8polyA (Figures 7B and 8A). However, mice injected with either AAV2/8DTAC or AAV2/8SACT had significantly less MAC deposition on both liver blood vessels and sinusoids relative to control (AAV2/8polyA)-injected mice (Figures 7C and 8B). Quantification of MAC staining intensity using ImageJ indicated a 56.7 ± 16.4% ($p = 0.0061$) reduction in human MAC

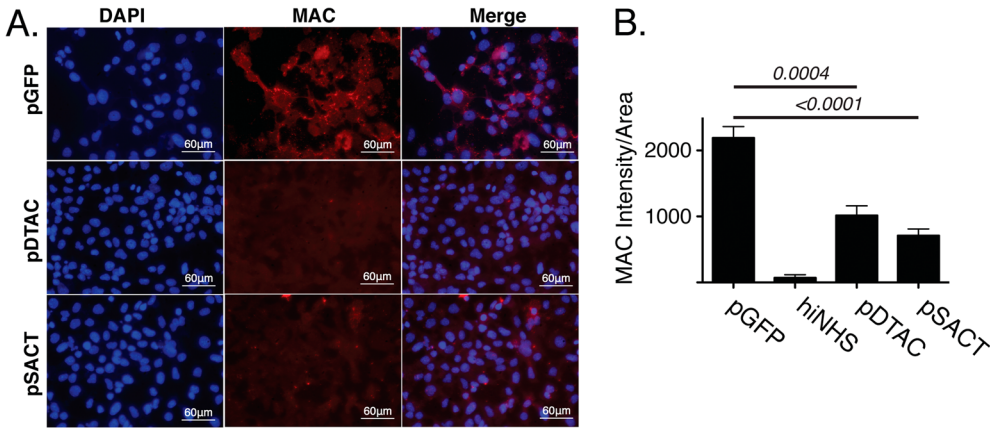

Figure 6. DTAC and SACT reduce deposition of the MAC *in vitro*. (A) Fluorescent micrographs of murine hepatocytes incubated with NHS in the presence of media from either pGFP-, pDTAC- or pSACT-transfected cells. Cells were stained with an antibody against MAC. A 4',6-diamidino-2-phenylindole (DAPI) stain is also shown. (B) Quantification of MAC staining intensity/area shows a 53.8 ± 10.37% ($p = 0.0004$, $n = 6$) and 67.8 ± 9.15% ($p < 0.0001$, $n = 6$) reduction in MAC deposition on murine hepatocytes incubated with media from cells transfected with either pDTAC and pSACT, respectively, relative to hepatocytes incubated with media from pGFP-transfected cells ($n = 6$). A control experiment of hepatocytes incubated with hiNHS in the presence of media from pGFP-transfected cells is also shown. The experiment was performed three times.

DOI: 10.1002/jgm

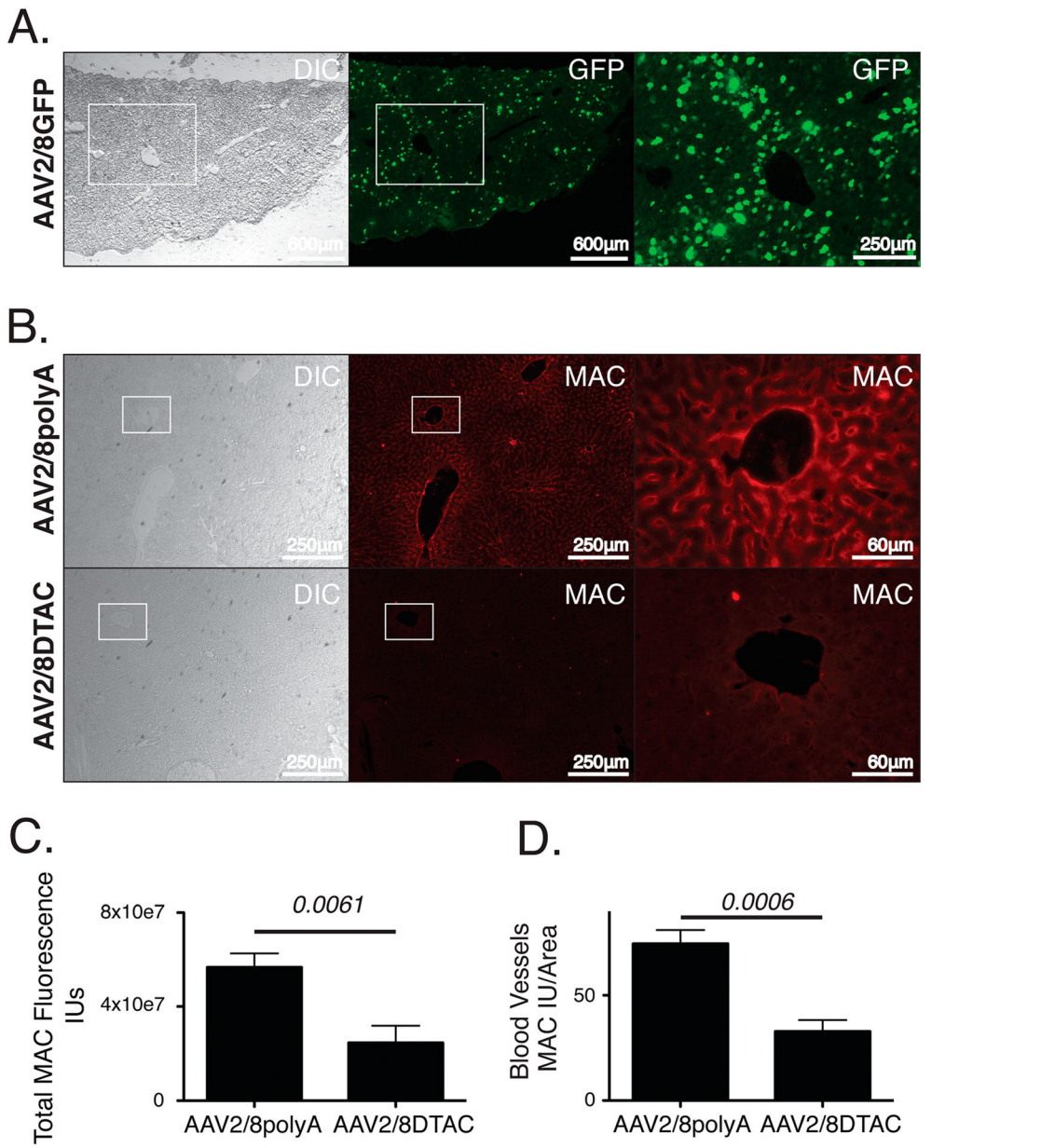

Figure 7. DTAC protects murine liver vasculature from human MAC deposition *in vivo* (A) Fluorescent micrographs of cryosections showing AAV2/8GFP transduction of murine liver. Efficient transduction is observed throughout the tissue. Higher magnification of the boxed region is shown. (B) Fluorescent micrographs of liver cryosections stained with anti-MAC antibody harvested from mice injected in the intraperitoneal space with either AAV2/8pA or AAV2/8DTAC and perfused with mPECAM1 antibody and NHS. Higher magnification of the boxed regions is shown. (C) Quantification of MAC staining intensity (IU) of liver sections shows a 56.7 ± 16.4% ($p = 0.0061$) reduction in human MAC deposition on the liver vasculature of AAV2/8DTAC-injected relative to AAV2/8polyA-injected mice. (D) Quantification of MAC staining intensity per area of blood vessels shows a 55.97 ± 11.34% ($p = 0.0006$) reduction in human MAC deposition in livers of AAV2/8DTAC-injected mice relative to AAV2/8polyA-injected. The assay was performed by injection of a total of six mice with AAV2/8pA and six mice with AAV2/8DTAC. The total number of mice was the result of two separate experiments. A total of eight independent sections per liver was stained and measured for MAC staining intensity for each mouse. GFP, green fluorescent protein; DIC, differential interference contrast; IU, intensity unit.

deposition on the liver vasculature of AAV2/8DTAC-injected relative to AAV2/8polyA-injected mice (Figure 7C). Similarly, AAV2/8SACT-injected animals showed a 63.2% ± 20.5% ($p = 0.0075$) reduction in human MAC deposition in their liver vasculature relative to AAV2/8polyA-injected mice (Figure 8B). Although endothelial cells of both the sinusoids and blood vessels indicated deposition of MAC, we were also specifically interested in the prevention of

DOI: 10.1002/jgm

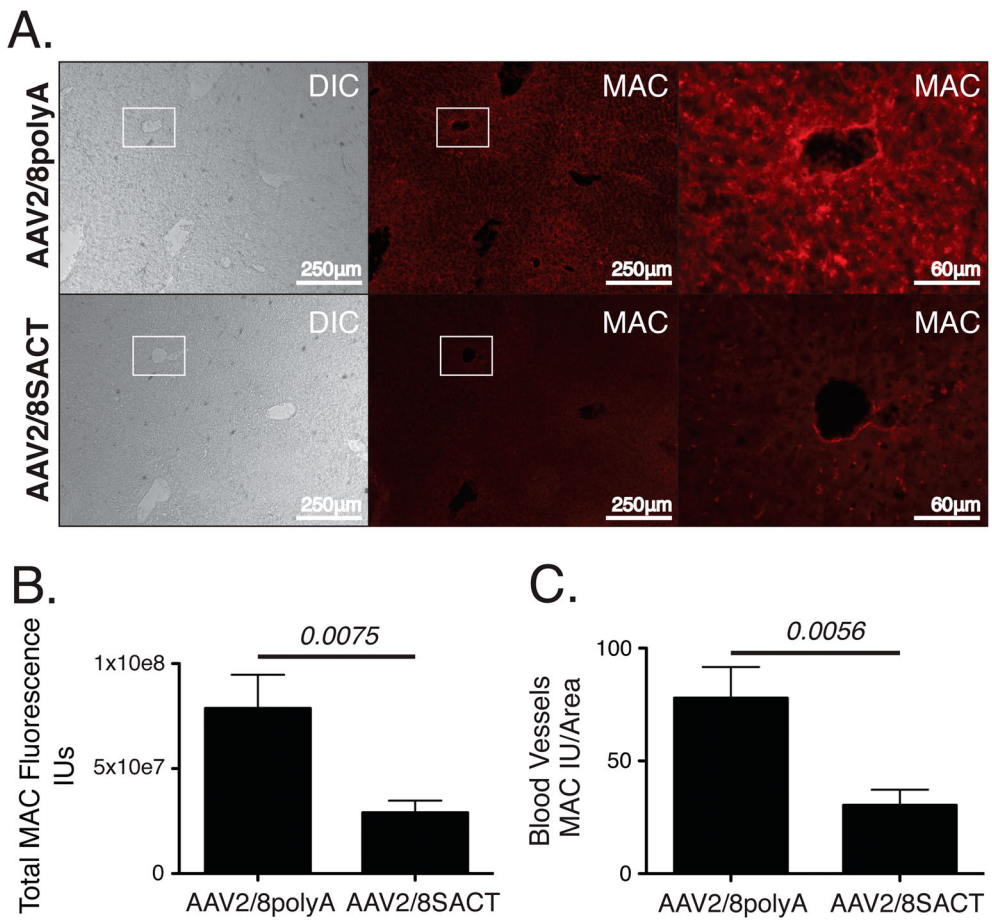

Figure 8. SACT protects murine liver vasculature from human MAC deposition *in vivo* (A) Fluorescent micrographs of liver cryosections stained with anti-MAC antibody harvested from mice injected in the intraperitoneal space with either AAV2/8pA or AAV2/8SACT and perfused with mPECAM1 antibody and NHS. Higher magnification of the boxed regions is shown. (B) Quantification of MAC staining intensity (IU) of liver sections shows a 63.2% ± 20.5% ($p = 0.0075$) reduction in human MAC deposition on the liver vasculature of AAV2/8SACT-injected relative to AAV2/8polyA-injected mice. (C) Quantification of MAC staining intensity per area of blood vessels shows a 61.1 ± 18.9% ($p = 0.0056$) reduction in human MAC deposition on the blood vessels of AAV2/8SACT-injected relative to AAV2/8polyA-injected mice. The assay was performed by injection of a total of eight mice with AAV2/8pA and nine mice with AAV2/8SACT. The total number of mice was the result of three separate experiments. A total of eight independent sections per liver was stained and measured for MAC staining intensity for each mouse. DIC, differential interference contrast; IU, intensity unit.

complement deposition on endothelial cells of the blood vessels. Quantification of larger (noncapillary) blood vessels of the liver indicated a significant reduction of 55.97 ± 11.34% ($p = 0.0006$) and 61.1 ± 18.9% ($p = 0.0056$) in human MAC deposition for AAV2/8DTAC- and AAV2/8SACT-injected animals, respectively, relative to AAV2/8polyA-injected animals (Figures 7D and 8C). We hence conclude that DTAC and SACT can provide significant protection to murine liver vasculature from activated human complement *in vivo*.

Discussion

In the present study, we describe a non-membrane associated recombinant molecule, SACT, that exhibits the combinatorial properties of CD46, CD55 and CD59. We determined that SACT is a secreted protein that can act as a co-factor for factor I mediated cleavage of C3b, accelerate the degradation of C3 convertase, attenuate recruitment of C9 into the MAC, protect cells from human complement mediated lysis and inhibit deposition of human MAC on mouse cells both *in vitro* and *in vivo*. Similarly, for DTAC, we observed the combined properties of CD55 and CD59 and DTAC did not, as anticipated, act as a co-factor for factor I mediated cleavage of C3b. The complement inhibitory effects for SACT and DTAC were all observed for a single dose of delivery vector *in vitro*. The assessment of a dose response in the present study was complicated by the need to use media from transfected cells. Higher concentrations of SACT and DTAC in the media would have to be achieved by increasing the plasmid

DOI: 10.1002/jgm

concentration in the transfection, an event that negatively impacts the integrity of the cells.

Complement is a critical first line of immune defense in vertebrates, affording protection against both foreign organisms and the threat of damaged self-cells [6]. Overexpression of complement regulators for the treatment of complement-mediated pathologies may pose risks as well as benefits. We chose therefore to inhibit the complement pathway at the combined points of C3 convertase formation and decay, as well as the formation of MAC, which has the advantage of allowing C1q to interact with modified self as well as nonself surfaces, permitting C3b-mediated phagocytosis offending cells and organisms [31]. Accordingly, we combined the functions of CD55, CD46 and CD59 into a single engineered protein, SACT. In addition, because CD46 functions at the level of C3b degradation, whereas CD55 prevents formation or accelerates the decay of convertases without altering C3b, we speculated that CD46 may interfere with C3b-mediated elimination of target cells. This may be especially important for the treatment of lupus-like diseases where reduced clearance of apoptotic cells can result in an autoimmune response to the dying cells [31]. Studies of the diversity of genetic factors involved in SLE, provide a comprehensive illustration of the importance of maintaining the potential for activation of upstream components of the cascade, at the same time as blocking downstream events [32]. We therefore generated and tested a second recombinant molecule that includes only CD55 and CD59 functions: DTAC.

In our studies, we utilized a gene therapy approach to deliver SACT or DTAC to cells in culture or to murine livers *in vivo*. Significant progress in the field of gene therapy indicates that this is a viable approach for the treatment of inherited or acquired diseases. Activation of complement plays a significant role in many disorders, including rheumatoid arthritis, a chronic disease of the complement system. Elevated levels of C3 and MAC and reduced levels of CD59 have been documented in the synovial tissue of rheumatoid arthritis patients [33,34]. These studies are further supported by the observation that injection of rat knee joints with monoclonal antibody against CD59 results in spontaneous and acute arthritis and an increase in joint pathology in $CD59^{-/-}$ mice, a phenotype that can be corrected by use of a membrane-targeted recombinant CD59 [35]. Attenuation of complement activation by targeting C5 was also found to be effective in a murine model of rheumatoid arthritis, suggesting that there are multiple points of the complement cascade that may serve as targets for complement based therapeutics [36]. In that context, SACT and DTAC may be particularly effective inhibitors of complement activation by virtue that they concomitantly target and attenuate various points of the complement cascade. Although repeat injection of inhibitors of complement activation into patients with rheumatoid arthritis would be feasible, a long-lasting single injection via gene therapy would be potentially preferred. AAV has been shown to persist in humans for years and for over a decade in large animals [37,38]. Furthermore, AAV is not associated with any known human disease.

A strong case for delivery of inhibitors of complement via a gene therapy approach may also be made for diseases such as AMD. Approximately 50% of patients that suffer from AMD have polymorphisms in the complement regulator factor H [39]. Individuals with an advanced form of AMD known as geographic atrophy have reduced levels of complement inhibitors on their RPE [40]. A commonly occurring polymorphism in C9 in the Japanese population that prevents those individuals from efficiently assembling MAC is protective against the progression of AMD, suggesting that inactivation of complement via a gene therapy approach may be a viable avenue for treatment of this disease [8]. However, all of the inhibitors of complement activation currently in clinical trials are small molecules, aptamers or antibodies that would need to be re-injected on a frequent basis into the eye of AMD patients [41]. This can lead to significant side effects such as increased intraocular pressure, endophthalmitis and retinal detachment [11,12]. A single injection that may produce a therapeutic protein locally for an extended time such as AAV mediated expression of SACT or DTAC may be particularly attractive for treatment of diseases such as AMD.

Although, in the present study, we described the first recombinant molecule that combines the properties of CD46, CD55 and CD59, our studies were inspired in part by earlier work. Previously, Fodor *et al.* [42] have described a membrane-associated recombinant molecule containing the combinatorial properties of CD55 and CD59. Similarly, Kroshus *et al.* [43] have described a soluble molecule combining the properties of CD46 and CD55 and demonstrated that this molecule could reduce acute cardiac tissue injury in a pig-to-human transplant model. Recently, a novel recombinant protein comprised of select domains from CR2 and factor H demonstrated increased survival, reduced autoantibody production and improved kidney function in a murine model of lupus [44]. However, in none of these studies was the recombinant protein delivered via a gene therapy approach.

Although AAV vectors are known to elicit a weak immune response *in vivo*, AAV serotypes 2 and 8 have been shown to induce complement-dependent activation of macrophages [45]. Interestingly, AAV2 interaction with complement did not result in activation of the complement cascade and the AAV8–immune interaction did not promote the production of neutralizing antibodies in wild-type mice *in vivo* [45,46]. One benefit of the use of

DOI: 10.1002/jgm

AAV8 as a gene delivery vector is that it has a substantially lower frequency of neutralizing antibodies in the human population when compared to AAV2 (3.8% versus 20%, respectively) [47]. Whether this is a result of reduced exposure of the population to AAV8 relative to AAV2, or a reduced ability of AAV8 relative to AAV2 to evoke a complement-dependent production of neutralizing antibodies, is not known. It is possible, however, that expression of SACT or DTAC from a recombinant AAV vector could negatively impact the production of neutralizing antibodies in the remaining population. This would be more likely to occur in the context of a rAAV8 vector, which, in contrast to rAAV2, has been shown to induce tolerance when injected intramuscularly in mice [46].

For our *in vivo* studies, we utilized AAV2 pseudotyped with AAV8 capsid (AAV2/8). This vector has been shown to have a very high efficiency of transduction of the liver of mice [48]. We chose to focus our *in vivo* studies in the liver in part because we have previously found that large amounts of human MAC can readily form on murine liver [27]. The liver was also selected in part because hepatocytes are responsible for the biosynthesis of 80–90% of the plasma components of complement [49]. Finally, the liver receives 25% of total blood flow, allowing for a potentially wide distribution of DTAC and SACT throughout the circulatory system, which would be relevant for the treatment of systemic disorders involving activation of complement [50]. Expression of DTAC and SACT *in vivo* revealed that both are potent inhibitors of human complement in an *in vivo* setting and our data lends support to their potential therapeutic value when secreted from the liver.

In summary, in the present study, we describe for the first time a novel non-membrane associated recombinant molecule, SACT, that exhibits the combinatorial properties of CD46, CD55 and CD59. We also describe DTAC that combines the combinatorial properties of CD55 and CD59. Each of these molecules was found to exhibit properties consistent with their modular structures and each of these molecules was a potent inhibitor of activation of complement *in vitro* and *in vivo*. These molecules are worthy of further study in animal models of complement-associated disorders.

Acknowledgements

The present study was supported by grants to R.K.S from The Ellison Foundation, The Virginia B. Smith Trust, The National Institute of Health/NEI (EY021805 and EY013837), The Department of Defense/TATRC and The Paul and Phyllis Fireman Foundation. The authors report that no competing financial interests or conflicts of interest exist.

References

1. Thurman JM, Renner B. Dynamic control of the complement system by modulated expression of regulatory proteins. *Lab Invest* 2011; **91**: 4–11.
2. Zipfel PF, Skerka C. Complement regulators and inhibitory proteins. *Nat Rev Immunol* 2009; **9**: 729–740.
3. Makrides SC. Therapeutic inhibition of the complement system. *Pharmacol Rev* 1998; **50**: 59–87.
4. Holers VM. The spectrum of complement alternative pathway-mediated diseases. *Immunol Rev* 2008; **223**: 300–316.
5. Mayilyan KR. Complement genetics, deficiencies, and disease associations. *Protein Cell* 2012; **3**: 487–496.
6. Walport MJ. Complement. First of two parts. *N Engl J Med* 2001; **344**: 1058–1066.
7. Mullins RF, Dewald AD, Streb LM, Wang K, Kuehn MH, Stone EM. Elevated membrane attack complex in human choroid with high risk complement factor H genotypes. *Exp Eye Res* 2011; **93**: 565–567.
8. Nishiguchi KM, Yasuma TR, Tomida D, *et al.* C9-R95X polymorphism in patients with neovascular age-related macular degeneration. *Invest Ophthalmol Vis Sci* 2012; **53**: 508–512.
9. Piccoli AK, Alegretti AP, Schneider L, Lora PS, Xavier RM. Expression of complement regulatory proteins CD55, CD59, CD35, and CD46 in rheumatoid arthritis. *Rev Bras Reumatol* 2011; **51**: 503–510.
10. Ricklin D, Lambris JD. Complement in immune and inflammatory disorders: therapeutic interventions. *J Immunol* 2013; **190**: 3839–3847.
11. Wu L, Martinez-Castellanos MA, Quiroz-Mercado H, *et al.* Twelve-month safety of intravitreal injections of bevacizumab (Avastin): results of the Pan-American Collaborative Retina Study Group (PACORES). *Graefes Arch Clin Exp Ophthalmol* 2008; **246**: 81–87.
12. Shima C, Sakaguchi H, Gomi F, *et al.* Complications in patients after intravitreal injection of bevacizumab. *Acta Ophthalmol* 2008; **86**: 372–376.
13. Ginn SL, Alexander IE, Edelstein ML, Abedi MR, Wixon J. Gene therapy clinical trials worldwide to 2012 – an update. *J Gene Med* 2013; **15**: 65–77.
14. Cashman SM, Ramo K, Kumar-Singh R. A non membrane-targeted human soluble CD59 attenuates choroidal neovascularization in a model of age related macular degeneration. *PLoS One* 2011; **6**: e19078.
15. Riley-Vargas RC, Gill DB, Kemper C, Liszewski MK, Atkinson JP. CD46: expanding beyond complement regulation. *Trends Immunol* 2004; **25**: 496–503.
16. Coyne KE, Hall SE, Thompson S, *et al.* Mapping of epitopes, glycosylation sites, and complement regulatory domains in human decay accelerating factor. *J Immunol* 1992; **149**: 2906–2913.
17. Kim DD, Song WC. Membrane complement regulatory proteins. *Clin Immunol* 2006; **118**: 127–136.
18. Ramo K, Cashman SM, Kumar-Singh R. Evaluation of adenovirus-delivered human CD59 as a potential therapy for AMD in a model of human membrane attack complex formation on murine RPE. *Invest Ophthalmol Vis Sci* 2008; **49**: 4126–4136.
19. Sweigard JH, Cashman SM, Kumar-Singh R. Adenovirus-mediated delivery of CD46 attenuates the alternative complement pathway on RPE: implications for age-related macular degeneration. *Gene Ther* 2011; **18**: 613–621.
20. Ma KN, Cashman SM, Sweigard JH, Kumar-Singh R. Decay accelerating factor (CD55)-mediated attenuation of complement: therapeutic implications for age-related macular degeneration. *Invest Ophthalmol Vis Sci* 2010; **51**: 6776–6783.
21. Fallaux FJ, Kranenburg O, Cramer SJ, *et al.* Characterization of 911: a new helper cell line for the titration and

propagation of early region 1-deleted adenoviral vectors. *Hum Gene Ther* 1996; **7**: 215–222.
22. Lublin DM, Liszewski MK, Post TW, *et al.* Molecular cloning and chromosomal localization of human membrane cofactor protein (MCP). Evidence for inclusion in the multigene family of complement-regulatory proteins. *J Exp Med* 1988; **168**: 181–194.
23. Zolotukhin S. Production of recombinant adeno-associated virus vectors. *Hum Gene Ther* 2005; **16**: 551–557.
24. Fagone P, Wright JF, Nathwani AC, Nienhuis AW, Davidoff AM, Gray JT. Systemic errors in quantitative polymerase chain reaction titration of self-complementary adeno-associated viral vectors and improved alternative methods. *Hum Gene Ther Methods* 2012; **23**: 1–7.
25. Happonen KE, Furst CM, Saxne T, Heinegard D, Blom AM. PRELP protein inhibits the formation of the complement membrane attack complex. *J Biol Chem* 2012; **287**: 8092–8100.
26. Johnson JB, Grant K, Parks GD. The paramyxoviruses simian virus 5 and mumps virus recruit host cell CD46 to evade complement-mediated neutralization. *J Virol* 2009; **83**: 7602–7611.
27. Gandhi J, Cashman SM, Kumar-Singh R. Soluble CD59 expressed from an adenovirus in vivo is a potent inhibitor of complement deposition on murine liver vascular endothelium. *PLoS One* 2011; **6**: e21621.
28. Ballard LL, Bora NS, Yu GH, Atkinson JP. Biochemical characterization of membrane cofactor protein of the complement system. *J Immunol* 1988; **141**: 3923–3929.
29. Satoh S, Terajima H, Yagi T, *et al.* Humoral injury in porcine livers perfused with human whole blood. *Transplantation* 1997; **64**: 1117–1123.
30. Anderson DH, Radeke MJ, Gallo NB, *et al.* The pivotal role of the complement system in ageing and age-related macular degeneration: hypothesis re-visited. *Prog Retin Eye Res* 2010; **29**: 95–112.
31. Trouw LA, Blom AM, Gasque P. Role of complement and complement regulators in the removal of apoptotic cells. *Mol Immunol* 2008; **45**: 1199–1207.
32. Karp DR. Complement and systemic lupus erythematosus. *Curr Opin Rheumatol* 2005; **17**: 538–542.
33. Kemp PA, Spragg JH, Brown JC, Morgan BP, Gunn CA, Taylor PW. Immunohistochemical determination of complement activation in joint tissues of patients with rheumatoid arthritis and osteoarthritis using neoantigen-specific monoclonal antibodies. *J Clin Lab Immunol* 1992; **37**: 147–162.
34. Konttinen YT, Ceponis A, Meri S, *et al.* Complement in acute and chronic arthritides: assessment of C3c, C9, and protectin (CD59) in synovial membrane. *Ann Rheum Dis* 1996; **55**: 888–894.
35. Williams AS, Mizuno M, Richards PJ, Holt DS, Morgan BP. Deletion of the gene encoding CD59a in mice increases disease severity in a murine model of rheumatoid arthritis. *Arthritis Rheum* 2004; **50**: 3035–3044.
36. Wang Y, Rollins SA, Madri JA, Matis LA. Anti-C5 monoclonal antibody therapy prevents collagen-induced arthritis and ameliorates established disease. *Proc Natl Acad Sci U S A* 1995; **92**: 8955–8959.
37. Colella P, Cotugno G, Auricchio A. Ocular gene therapy: current progress and future prospects. *Trends Mol Med* 2009; **15**: 23–31.
38. Jiang H, Couto LB, Patarroyo-White S, *et al.* Effects of transient immunosuppression on adenoassociated, virus-mediated, liver-directed gene transfer in rhesus macaques and implications for human gene therapy. *Blood* 2006; **108**: 3321–3328.
39. Klein RJ, Zeiss C, Chew EY, *et al.* Complement factor H polymorphism in age-related macular degeneration. *Science* 2005; **308**: 385–389.
40. Ebrahimi KB, Fijalkowski N, Cano M, Handa JT. Decreased membrane complement regulators in the retinal pigmented epithelium contributes to age-related macular degeneration. *J Pathol* 2013; **229**: 729–742.
41. Keane PA, Sadda SR. Development of anti-VEGF therapies for intraocular use: a guide for clinicians. *J Ophthalmol* 2012; **2012**: 483034.
42. Fodor WL, Rollins SA, Guilmette ER, Setter E, Squinto SP. A novel bifunctional chimeric complement inhibitor that regulates C3 convertase and formation of the membrane attack complex. *J Immunol* 1995; **155**: 4135–4138.
43. Kroshus TJ, Salerno CT, Yeh CG, Higgins PJ, Bolman RM, Dalmasso AP. A recombinant soluble chimeric complement inhibitor composed of human CD46 and CD55 reduces acute cardiac tissue injury in models of pig-to-human heart transplantation. *Transplantation* 2000; **69**: 2282–2289.
44. Sekine H, Kinser TT, Qiao F, *et al.* The benefit of targeted and selective inhibition of the alternative complement pathway for modulating autoimmunity and renal disease in MRL/lpr mice. *Arthritis Rheum* 2011; **63**: 1076–1085.
45. Zaiss AK, Cotter MJ, White LR, *et al.* Complement is an essential component of the immune response to adeno-associated virus vectors. *J Virol* 2008; **82**: 2727–2740.
46. Mays LE, Wang L, Lin J, *et al.* AAV8 induces tolerance in murine muscle as a result of poor APC transduction, T cell exhaustion, and minimal MHCI upregulation on target cells. *Mol Ther* 2014; **22**: 28–41.
47. Gao GP, Alvira MR, Wang L, Calcedo R, Johnston J, Wilson JM. Novel adeno-associated viruses from rhesus monkeys as vectors for human gene therapy. *Proc Natl Acad Sci U S A* 2002; **99**: 11854–11859.
48. Paneda A, Vanrell L, Mauleon I, *et al.* Effect of adeno-associated virus serotype and genomic structure on liver transduction and biodistribution in mice of both genders. *Hum Gene Ther* 2009; **20**: 908–917.
49. Qin X, Gao B. The complement system in liver diseases. *Cell Mol Immunol* 2006; **3**: 333–340.
50. Myers JD, Hickam JB. An estimation of the hepatic blood flow and splanchnic oxygen consumption in heart failure. *J Clin Invest* 1948; **27**: 620–627.